International Journal of
Composite Materials and Matrices

ISSN: 2582-435X
Volume 10, Issue 2, 2024
DOI (Journal): 10.37628/IJCMM

https://journals.stmjournals.com/ijcmm/

Review | ijcmm

One-Step Fabrication of Superomniphobic Pvdf-HFP-SiO_2 Membrane for Long-Term CO_2 Absorption in Membrane Gas Absorption System

Yee Jack Lai Yong Jie[1], Pei Ching Oh[1,*], Loo Thiam Leng Chew [2], Abdul Latif Ahmad[3]

Abstract

Membrane pore wetting is one of the major challenges for membrane gas absorption, especially when low surface tension liquid absorbents such as amine absorbents are utilized. To minimize diffusion resistance across the membrane, maintaining a non-wetted operating mode in membrane gas absorption is crucial. In this study, a superomniphobic polyvinylidene fluoride-co-hexafluoropropylene membrane was fabricated by adding silica nanoparticles (SiO_2) in an ethanol coagulation bath through non-solvent-induced phase separation. The surface properties and long-term CO_2 absorption performance in membrane gas absorption system was analyzed. The incorporation of SiO_2 contributed to the formation of a hierarchical structure composed of microscale polymer spherulites and nanoscale SiO_2. The fabricated membrane achieved water and methyldiethanolamine contact angles of 160.28° and 152.11°, respectively. Long-term CO_2 absorption stability experiments were conducted by immersing the synthesized membrane in methyldiethanolamine solution for 0, 3, and 6 days. Compared to the pristine membrane, the superomniphobic membrane was able to sustain 81.88% and 74.44% of CO_2 absorption flux after 3 days and 6 days of methyldiethanolamine immersion, respectively, which can be attributed to the improved wetting resistance.

Keywords: Superomniphobic surfaces, liquid repelling properties, CO_2 absorption, membrane gas absorption, gas–liquid contact

INTRODUCTION

***Author for Correspondence**
Pei Ching Oh
E-mail: peiching.oh@utp.edu.my

[1]Department of Chemical Engineering, Universiti Teknologi PETRONAS, Seri Iskandar, Perak, Malaysia.
[2]CO2 Research Centre (CO2RES), Institute of Contaminant Management, Universiti Teknologi PETRONAS, Seri Iskandar, Perak, Malaysia.
[3]School of Chemical Engineering, Engineering Campus, Universiti Sains Malaysia, Nibong Tebal, Pulau Pinang, Malaysia.

Received date: August 05, 2024
Accepted date: September 30, 2024
Published date: November 30, 2024

Citation: Yee Jack Lai, Yong Jie Loo, Pei Ching Oh, Thiam Leng Chew, Abdul Latif Ahmad. One-Step Fabrication of Super Omni Phobic Pvdf-HFP-SiO2 Membrane for Long-Term CO_2 Absorption in Membrane Gas Absorption System. International Journal of Composite Materials and Matrices 2024; 10(2): 35–44.

CO_2 capture using membrane gas absorption (MGA) or gas–liquid contacting system, a combination of membrane separation and chemical absorption has been extensively investigated by researchers as it can potentially offer smaller capital cost and energy consumption compared to traditional CO_2 absorption column [1]. In the MGA system, the membrane serves as a non-selective contacting medium that provides a large surface area for the interaction between liquid adsorbent and gas stream without direct contact. With transmembrane pressure difference, CO_2 in the natural gas or biogas diffuses across the membrane pores and is absorbed by the liquid absorbent. Studies have shown that liquid absorbent stream pressure is higher than gas stream pressure during membrane contact absorption, which causes liquid

absorbent to enter and wet the membrane pores easily [2]. In addition, polymeric membranes' poor chemical resistance [3], large pore size [4], and their weak compatibility with absorbents often result in severe wetting due to morphological changes such as membrane swelling [5]. The morphological changes affect the pore size of the used membrane, decreasing the surface contact angle with liquid and hence more vulnerable to wetting. Therefore, maintaining a non-wetting operation mode, where the pores remain gas-filled, is crucial for achieving high and steady CO_2 mass transfer flux [6] throughout the whole MGA process. To enhance the liquid-repelling properties of membranes, fluoropolymers; especially polytetrafluoroethylene, polychlorotrifluoroethylene, polyvinylidene fluoride, and its copolymers emerged as the preferred base materials [7] for liquid-repelling membranes. The fluorinated chains within CF_3 functional groups present in the substances exhibit weak Van der Waals force, resulting in low cohesive energy and surface tension [8].

Previous studies have focused on designing hydrophobic and superhydrophobic membranes using fluorinated materials combined with liquid-repelling additives to address membrane pore-wetting issues in MGA. These materials and additives increase surface roughness and reduce surface energy, thereby decreasing pore-wetting tendency by trapping air pockets between liquid droplets and the rough structures formed [9,10]. Li et al. [11] modified commercial PTFE membrane by spray-coating them with hydrophobic fumed silica and methyl ethyl ketone (MEK) on the membrane surface. After spray deposition, the water contact angle and sliding angle of the PTFE membrane improved significantly, from 117.2° to 158.4° and from 42.3° to 1.3°, respectively. The modified membrane was able to withstand operating pressure up to 10 bars and achieved 97.1% CO_2 removal efficiency. Similarly, Toh et al. [12] developed a superhydrophobic PVDF-HFP mixed matrix membrane by incorporating polydimethylsiloxane-grafted-silica nanoparticles in the polymer matrix before membrane casting with non-solvent-induced phase separation. Blending PGS nanoparticles in the polymer matrix resulted in rough micro- and nano-scale hierarchical structures and reduced surface energy. The resulting membrane achieved a contact angle of 149.87° with water and 130° with monoethanolamine (MEA). It exhibited only a 22% declination for CO_2 mass transfer flux after 12 days of pre-immersion in MEA and 150 h of MGA operation. The studies have shown that improving surface liquid repelling properties of membrane can enhance the overall performance of MGA, including its long-term stability.

To date, membrane wetting remains one of the primary challenges faced in the MGA system. Although the membranes used in gas absorption are typically hydrophobic and designed to resist pores wetting, liquid absorbents with low surface tension especially alkonoamines can still penetrate through the membrane pores and reduce CO_2 absorption flux after prolonged operation [13]. To promote further improvements in the long-term stability of MGA, omniphobic and superomniphobic membranes that can repel low surface tension liquid received great attention. Huang et al. [14] reported the fabrication of an omniphobic membrane by depositing zinc oxide (ZnO) nanoparticles and conducting surface fluorination with 1H, 1H, 2H, and 2H-perfluorodecyltriethoxysilane (FAS 17). The ZnO nanoparticles coating layer enhanced the surface roughness and formed hierarchical structure whereas surface fluorination reduces surface free energy. The fabricated omniphobic membrane surface showed a contact angle of 147.8° with absorbent amine and maintained steady absorption flux throughout the whole operating period up to 96 h. In addition, omniphobic and superomniphobic membranes also demonstrated outstanding performance in oily wastewater separation [15–20]. The excellent results in membrane distillation suggest the high potential for superomniphobic membranes in MGA application as well. Despite the excellent liquid-repelling properties and high potential for MGA application, there have been limited studies conducted to investigate the implementation of oil-repelling membranes in CO_2 absorption via the MGA system, especially for superomniphobic membranes. Nonetheless, the development of superomniphobic membranes is more challenging compared to superhydrophobic membranes as it often involves the combination of multiple complex surface modification approaches [21–24]. According to the problems analyzed in Erbil's review article [25], a single-step fabrication method that is feasible for

large-scale productions is required for liquid-repelling surfaces to be applied in industry.

In this work, one-step non-solvent induced phase inversion was adopted as the modification method to enhance surface liquid repelling properties. The effect of silica (SiO_2) nanoparticles was studied by incorporating them in a coagulation bath as a non-solvent additive during the fabrication of polyvinylidene fluoride-co-hexafluoropropylene (PVDF-HFP) membrane. The surface morphology and liquid-repelling properties were characterized. The CO_2 absorption performance was evaluated in the MGA system by employing methyldiethanolamine (MDEA) as the liquid absorbent.

EXPERIMENTAL

Materials

The membrane base material, PVDF-HFP in pellet form (Mw 400,000, Mw/Mn 130,000) was purchased from Sigma Aldrich and used in the fabrication of the membrane. N-methyl-2-pyrrolidone (NMP, >99.5%) supplied by Millipore was used as the solvent to dissolve PVDF-HFP pellets during the preparation of dope solution. LUDOX HS-40 colloidal silica nanoparticles (density 1.3 g/ml, specific surface area 220 m^2/g) were supplied from Sigma Aldrich. Meanwhile, ethanol (>95%) and MDEA supplied from R&M Chemicals, Malaysia were used as the coagulation bath (non-solvent) during the fabrication of membrane and liquid absorbents in the MGA system, respectively. All materials were used without further purification.

Fabrication of PVDF-HFP Silica Membrane

The membranes were fabricated via a non-solvent-induced phase separation (NIPS) process. 15wt% (or 1.65 g) of PVDF-HFP pellets were dried in a vacuum oven at 70°C for 12 h to remove moisture. Afterward, the polymer pellets were gradually added into 9.07 ml NMP solvent at 70°C followed by magnetically stirring until a homogenous dope solution was obtained. The dope solution was degassed in an ultrasonic bath for 5 h to remove trapped bubbles and left standing overnight. The polymer dope solution was poured onto a clean glass substrate and cast using a casting blade at a 200 μm thickness gap. Before casting, 0.06 wt%, 0.12 wt%, and 0.18 wt% [26] of LUDOX HS-40 SiO_2 nanoparticles were dispersed in an ethanol coagulation bath until a homogenous solution was obtained. Then, the membrane films were immersed in the prepared SiO_2 nanoparticles/ethanol bath immediately for 24 h to induce solvent/non-solvent exchange. The corresponding samples were named M-0.06, M-0.12, and M-0.18, respectively. After 24 h of immersion, the membrane films were transferred into a water bath for at least 30 min to remove excess solvent. Finally, the membranes were dried at room temperature.

Membrane Characterizations

The surface and cross-section morphology of the membrane samples were observed with scanning electron microscopy (Zeiss EVO LS15 SEM with EDS) at 15 kV accelerating voltage and 1–3K magnification. Each sample was sputtered with gold or platinum for 15 seconds at 40 mA before the test to mitigate the charging effect, which is known to produce image artifacts that can lead to abnormal contrast and image distortion.

Elemental mapping at the membrane surface was conducted using an energy-dispersive X-ray spectrometer (EDS) (Zeiss EVO LS15 SEM with EDS) to study the elemental composition of the membrane surface before and after incorporating silica nanoparticles.

The sessile drop technique was applied to measure the contact angle of the membranes' outer surface by using a goniometer (Rame-Hart, Model: 260-F4). For each measurement, 5 μL of water or MDEA solution was dropped on the membrane surface with a microsyringe at room condition. A digital video image was taken by a camera and the contact angle readings were determined by Dropmeter software. To minimize errors, three measurements on different spots of the same

membrane surface were taken to obtain the average reading.

Membrane CO_2 Gas Absorption Test

To study the wetting resistance and long-term operational stability of the membrane, the membranes were pre-immersed in MDEA solution for 0, 3, and 6 days before the MGA CO_2 absorption experiment. The CO_2 absorption test was performed using an MGA setup at room temperature and atmospheric pressure. The membrane module was filled with a membrane sample (radius 3.4 cm). Pure CO_2 gas was used as the feed gas, with its flow rate controlled and determined by a mass flowmeter, whereas 1.5M MDEA solution was used as the liquid absorbent. The membrane was subjected to 120 ml/min of pure CO_2 feed on the top surface and 120 ml/min of MDEA solution on the bottom surface at a countercurrent direction. Before taking measurements, the system was stabilized for at least 30 minutes to achieve a steady state. Upon reaching a steady state, outlet CO_2 flowrate was measured with a bubble flowmeter and the CO_2 absorption flux can be calculated using Equation (1):

$$J = \frac{(Q_{g,i} - Q_{g,o})\rho_g}{M_g A}, \quad (1)$$

where $Q_{g,i}$ and $Q_{g,o}$ denote the inlet and outlet flow rates of carbon dioxide gas (ml/min), respectively, ρ_g represents the density of CO_2 gas (g/ml), M_g represents the molecular weight of CO_2 gas (g/mol), and A represents the effective contacting area of the membrane (m^2).

RESULT AND DISCUSSION

Surface Morphology

SEM imaging was conducted to provide visualization of the structure of the membrane's top surface and cross-section. Figure 1 shows an SEM image of pristine PVDF-HFP membrane and membranes prepared with different concentrations of silica nanoparticles added in an ethanol coagulation bath. The cross-section image shown in Figure 1(a) displayed skinless and uniform spherulitic structures distributed across the entire pristine membrane surface with very little macrovoid formation. In Figure 1(b), the pristine PVDF-HFP membrane fabricated using ethanol as a coagulation bath showed pores and particulate-like morphology on the interlinking polymer globules. This was due to the use of pure ethanol in the coagulation bath, which delayed the precipitation of the membrane by slowing down the exchange rate between solvent and non-solvent [27, 28]. The poor coagulation ability of ethanol bath impeded the exchange process and allowed a great extent of polymer crystallization to occur in the immersion process. The findings highlighted the significant role of weak non-solvents such as ethanol in determining the membrane structure during the membrane fabrication process.

Figure 1(c–h) visualizes the effect of silica nanoparticles in the ethanol coagulation bath on membrane morphology. Upon addition of SiO_2 nanoparticles, their deposition was visible as white spots that scattered over the polymer spherulites. The top surface of the M-0.06 membrane shown in Figure 1(d) appeared relatively smooth with minimal structural change compared to M-0.12 and M-0.18. As the concentration of silica nanoparticles increased to 0.12 wt%, the top surface (Figure 1(f)) exhibited a significantly greater number of rough and fine features. At 0.18 wt%, the top surface image (Figure 1(h)) displayed a more well-defined and textured structure morphology with interconnected porous polymer globules, characterized by a more pronounced presence of silica nanoparticles. After incorporating silica nanoparticles in a coagulation bath, M-0.06, M-0.12, and M-0.18 exhibited noticeable attachment of silica nanoparticles by having denser and more compact spherulitic structured surfaces covered with lumps. The membranes acquired a hierarchical structure consisting of microscale polymer crystalline and nanoscale silica nanoparticles. According to Wu et

al. [29], the formation of dense structures was due to the deposition of silica nanoparticles on the polymer globules. This could be explained by the migration of the silica nanoparticles from the coagulation medium onto the polymer film during solvent/non-solvent exchange. However, the surface morphological images revealed a small degree of silica nanoparticle agglomeration, likely resulting from uneven deposition on the membrane surface [30]. Overall, the deposition of these nanoparticles formed multilevel protrusions that were densely distributed on the membrane surface, resulting in the formation of a bumpy surface composed of nanoparticle clusters.

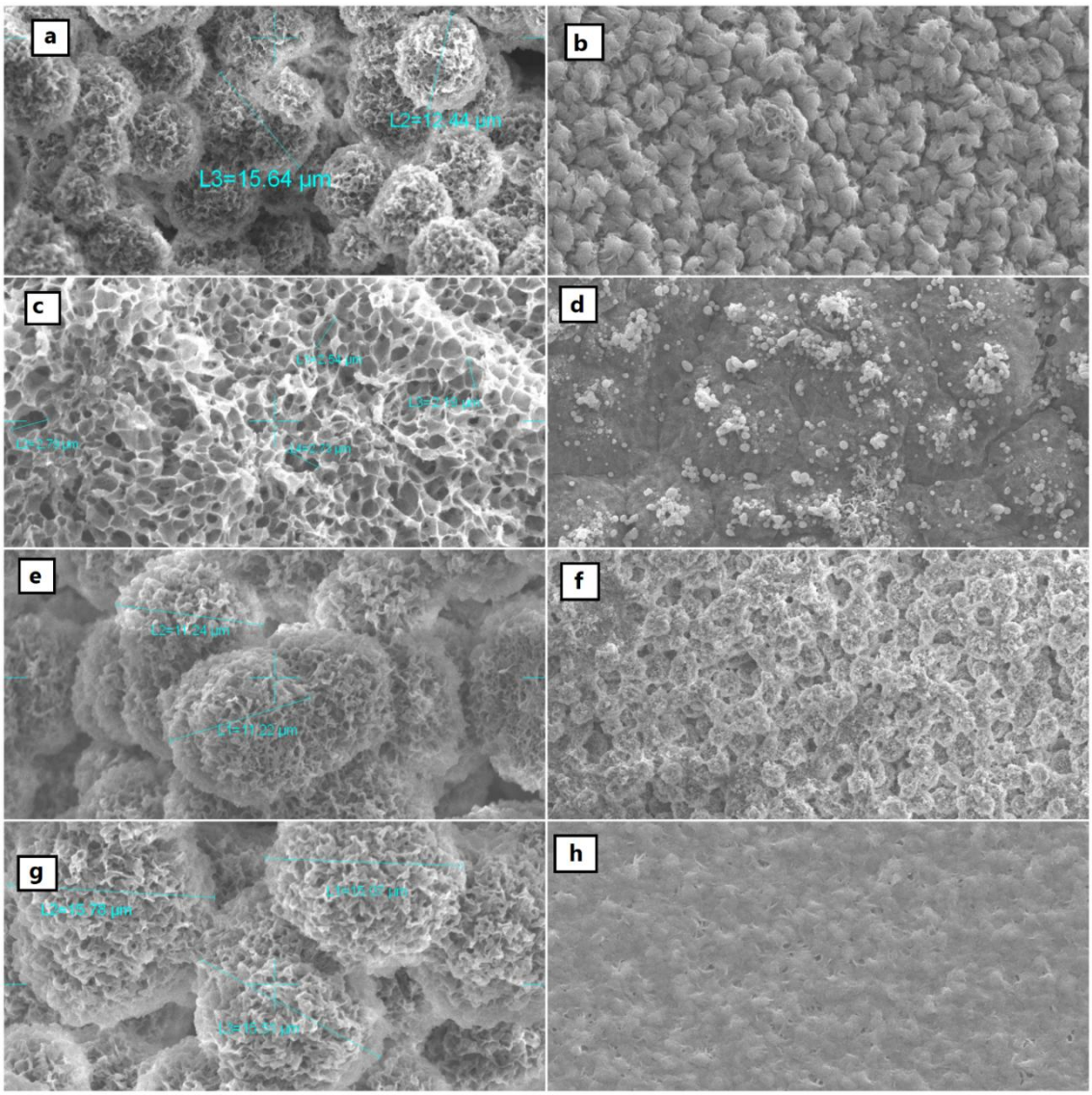

Figure 1. SEM images of (a, b) pristine membrane, (c, d) M-0.06, (e, f) M-0.12, (g, h) M-0.18. The left images display the cross-section surface structure, whereas the right images display the top surface structure.

Elemental Analysis

The elemental composition of the pristine membrane, M-0.06, M-0.012, and M-0.018 were tested using energy dispersive X-ray (EDX) analysis. Table 1 presents the weight percentages of carbon (C), fluorine (F), and silicon (Si). Carbon and fluorine are contributed by PVDF-HFP, while silicon is contributed by silica nanoparticles. As the silica nanoparticles concentration increased from 0.06 wt% to 0.18 wt%, greater silicon content was identified on the membrane surface, accompanied by a

reduction in fluorine content. The increasing silicon content signified the successful deposition of silica nanoparticles on the membrane surfaces.

Table 1. Elemental analysis of membranes.

Membrane	Elemental Analysis		
	C	F	Si
Pristine	44.73	55.27	–
M-0.06	44.36	55.32	0.32
M-0.12	44.61	54.97	0.42
M-0.18	43.76	55.65	0.59

Contact Angle Measurement

Contact angle analysis that is correlated with the long-term stability of membrane was employed to evaluate the superomniphobicity of the membranes after being incorporated with various concentrations of LUDOX HS-40 silica nanoparticles. Apart from testing water contact angles, the membrane surfaces were also tested with low surface tension amine absorbent that is commonly used in MGA applications, MDEA. The initial water and MDEA contact angle of pristine PVDF-HFP membrane were found at 110.15° and 86.81°, respectively. Referring to Figure 2, M-0.06 had a significant improvement in contact angle of 131.14° with water and 110.16° with MDEA due to the incorporation of silica nanoparticles in the coagulation bath. According to Wu et al. [29], the addition of hydrophobic modified SiO_2 nanoparticles (HMSNs) in the coagulation bath resulted in higher contact angles for water, glycerol, and diiodomethane compared to pristine PVDF membrane. Upon increasing silica nanoparticles concentration to 0.18 wt%, significant enhancement in water and MDEA contact angle was noticed, in which the water contact angle reached 160.28° while the MDEA contact angle reached 152.11°, indicating enhanced anti-wettability. The membrane successfully achieved superomniphobicity.

The significant rise in contact angle was attributed to the low surface energy from the high fluorine content and the multiscale hierarchical structures created by coating with silica nanoparticles. A decrease in surface energy corresponds to the reduced affinity of liquid molecules for the membrane surface [16,31] whereas roughness on the hierarchical surface entraps multiple air pockets underneath, reducing direct contact between liquid droplets and the membrane surface [32]. As a result, M-0.18 is preferable for CO_2 absorption in the MGA system.

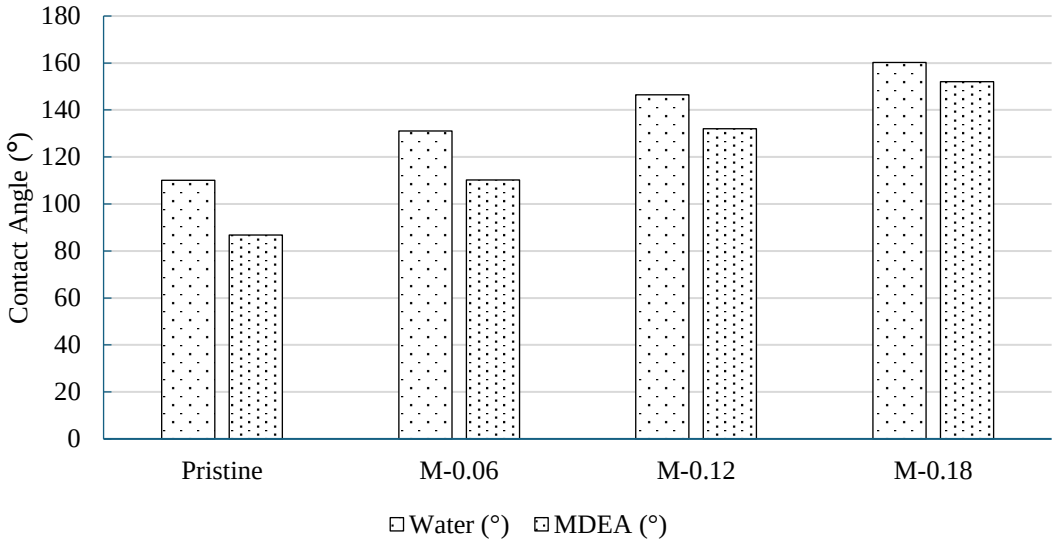

Figure 2. Contact angle measurement of membranes using water and MDEA.

MGA Test

CO_2 absorption flux of the pristine membrane and modified membrane with the largest wetting resistance (M-0.18) were compared during the MGA test. Since pore wetting occurs in the long-term [33], the tested membranes were pre-immersed in MDEA solution for 0, 3, and 6 days before conducting the MGA test to study the deterioration of CO_2 absorption flux resulting from membrane pore-wetting. The impacts of different immersion periods on the CO_2 absorption flux of both membranes are illustrated in Figure 2. Without pre-immersion (0-day immersion in MDEA solution), M-0.18 exhibits a higher CO_2 absorption flux of 0.002616 mol/m²·s compared to the pristine membrane, which has a flux of 0.000914 mol/m²·s. The enhancement in the absorption flux of M-0.18 indicated that the addition of silica nanoparticles on the membrane surface did not significantly increase its resistance to gas transport. Due to the better wetting resistance of M-0.18, pore wetting was delayed as the penetration of liquid absorbent into the membrane pores was more challenging than the pristine membrane. On the other hand, the liquid absorbent penetrated the pristine membrane pores after 30 minutes, increasing CO_2 mass transfer resistance.

After 3 days of MDEA immersion, obvious pore-wetting effects were observed from substantial CO_2 absorption flux drop of both studied membranes. The pristine membrane experienced a notable reduction in absorption flux, dropping from 0.000914 mol/m^{2}s to 0.000500 mol/m^{2}s, equating to a 45.30% decrease in performance. Prolonged contact of pristine PVDF-HFP membrane with amine absorbent-induced degradation and changes results in porosity, pore size, wetting resistance, and other surface properties [34, 35]. In contrast, M-0.18 showed better operational stability than pristine membranes. The results demonstrated that M-0.18 experienced a comparatively smaller percentage drop of CO_2 flux, from 0.002616 mol/m^{2}s to 0.002142 mol/m^{2}s and was able to sustain 81.88% of the original performance.

A further decline in performance was observed in both membranes after 6 days of immersion in MDEA solution. For pristine membranes, the absorption flux experienced a further 57% drop from 3-day to 6-day immersion, from 0.000500 mol/m^{2}s to 0.000215 mol/m^{2}s. The absence of additional silica nanoparticles in the pristine membrane caused it to be more vulnerable to cumulative effects of wetting as more amine absorbent penetrated can easily penetrate through an extended period of immersion, causing further performance decline. Meanwhile, M-0.18 exhibited a lower rate of membrane degradation, with a further reduction of only 25.6%, from 0.002142 mol/m^{2}s to 0.001593 mol/m^{2}s. Superomniphobicity that has excellent wetting resistance towards low surface tension amine absorbent hinders amine absorbent from entering the pores, minimizing structural and morphological change of membrane resulting from wetting. This demonstrated the effect of superomniphobicity on the operational stability of the membrane in MGA and dictated the feasibility of improving long-term stability of the membrane using a one-step addition of SiO_2 nanoparticles in a coagulation bath.

The CO_2 flux of the synthesized membrane in this work was compared in Table 2 with commercial and in-house made PVDF membranes. It was observed that the CO_2 absorption flux of M-0.18 was slightly higher than the membranes in the work reported by Ahmad et al. [36], Chang et al. [37], and Pang et al. [38]. This may be attributed to M-0.18's better wetting resistance towards low surface tension liquid absorbents such as MDEA and MEA, which could be observed from water and liquid absorbent contact angle. Comparing M-0.18 with the commercial PVDF membrane supplied by Memcore Australia in Rongwong's work [39], there was only a very small difference in CO_2 absorption flux when similar liquid absorbents were used, which indicates that the surface modification method used in this work does not significantly reduce CO_2 flux. Overall, the membrane fabricated in this work demonstrated excellent MGA performance for a prolonged duration with comparable CO_2 flux with other PVDF membranes.

Table 2. Comparison of the membrane performance with literature.

Polymer	Additives	Contact Angle (°)	Liquid Absorbent	CO_2 flux (mol/m^{2}s)	Reference
Commercial PVDF	–	–	Distilled water	1.1×10^{-3}	[40]
Commercial	–	92° with water	MEA	4×10^{-3}	[39]

PVDF					
PVDF	Trisilanolisobutyl POSS	132.4° with water	Distilled water	7.68×10^{-4}	[36]
PVDF mixed matrix membrane	Multi-walled carbon nanotube (MWCNT)	103° with water	Distilled water	2.8×10^{-3}	[41]
PVDF mixed matrix membrane	Hydrophobic LDPE coated with silica nanoparticles	111.8° with water	MEA	2.4×10^{-3}	[37]
PVDF mixed matrix membrane	Hexadecyltrimethoxysilane	160° with water, 158° with DEA	DEA	2.39×10^{-3}	[38]
PVDF-HFP	Silica nanoparticles	160.28° with water, 152.11° with MDEA	MDEA	2.6×10^{-3}	This work

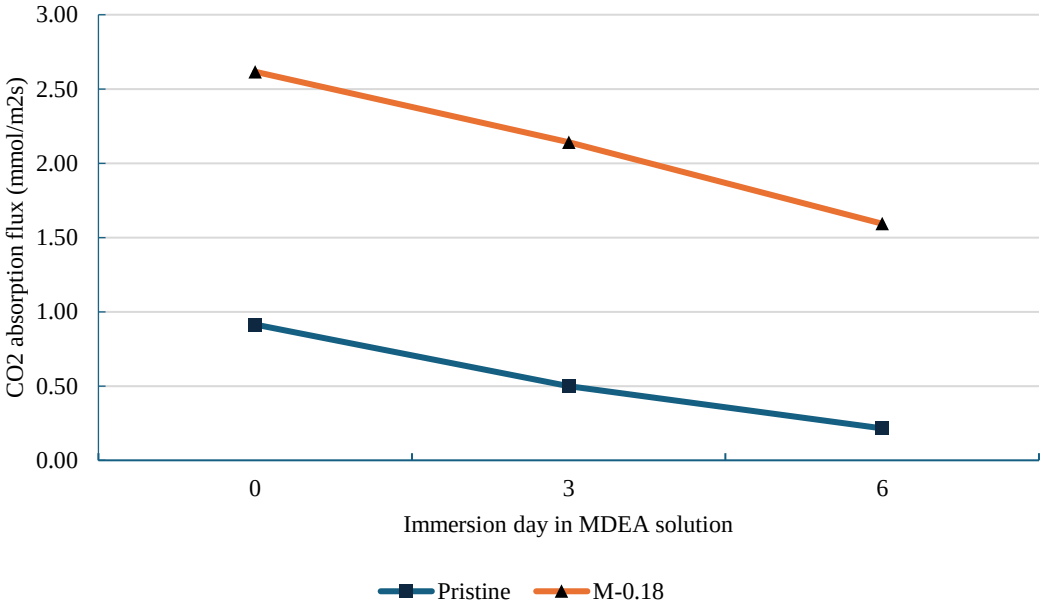

Figure 3. CO_2 flux of pristine and M-0.18 membrane over 0-day, 3-day, and 6 days of immersion in MDEA solution.

CONCLUSIONS

In conclusion, this study demonstrated a simple and straightforward non-solvent induced phase inversion method to design superomniphobic PVDF-HFP membranes. By forming hierarchical surface roughness and low surface free energy through the addition of silica nanoparticles, the resultant membrane revealed outstanding surface liquid-repelling properties, characterized by a high contact angle that prevented penetration of water and amine absorbent droplets. The prepared membrane achieved a CO_2 absorption flux of 2.6×10^{-3} mol/m^2s and sustained reasonable absorption flux after 6 days of immersion in amine absorbent. Compared with the pristine membrane, the addition of silica nanoparticles in the coagulation bath enhanced the long-term stability and absorption performance of the PVDF-HFP membrane. Overall, the simplicity and effectiveness of the fabrication method used in the study are crucial for the future development of superomniphobic membranes to effectively address the membrane pore wetting problem encountered in MGA operation and to scale up to industry scale.

ACKNOWLEDGMENT

This research work was supported by the Fundamental Research Grant Scheme (FRGS grant no. FRGS/1/2022/TK05/UTP/02/16 Cost Center 015MA0-150) and CO_2 Research Centre (CO2RES).

DECLARATION OF COMPETING INTEREST

The authors declare that they have no known competing financial interests or personal relationships that could have appeared to influence the work reported in this paper.

REFERENCES

1. Imtiaz A, Othman MH, Jilani A, Khan IU, Kamaludin R, Ayub M, et al. A critical review in recent progress of hollow fiber membrane contactors for efficient CO2 separations. Chemosphere. 2023;325:138300.
2. Zhang Y, Sunarso J, Liu S, Wang R. Current status and development of membranes for CO2/CH4 separation: a review. Int J Greenhouse Gas Contr. 2013;12:84–107.
3. Lin YF, Wang CS, Ko CC, Chen CH, Chang KS, Tung KL, et al. Polyvinylidene fluoride/siloxane nanofibrous membranes for long-term continuous CO2-capture with large absorption-flux enhancement. ChemSusChem. 2014;7(2):604–9.
4. Boo C, Lee J, Elimelech M. Omniphobic polyvinylidene fluoride (PVDF) membrane for desalination of shale gas produced water by membrane distillation. Environ Sci Technol. 2016;50(22):12275–82.
5. Barbe AM, Hogan PA, Johnson RA. Surface morphology changes during initial usage of hydrophobic, microporous polypropylene membranes. J Membr Sci. 2000;172(1–2):149–56.
6. Mosadegh-Sedghi S, Rodrigue D, Brisson J, Iliuta MC. Wetting phenomenon in membrane contactors–causes and prevention. J Membr Sci. 2014;452:332–53.
7. Kota AK, Kwon G, Tuteja A. The design and applications of superomniphobic surfaces. NPG Asia Mater. 2014;6(7):e109.
8. Hare EF, Shafrin EG, Zisman WA. Properties of films of adsorbed fluorinated acids. J Phys Chem. 1954;58(3):236–9.
9. Cassie AB, Baxter S. Wettability of porous surfaces. Transac Faraday Soc. 1944;40:546–51.
10. Verma J, Bennett GJ, Goel S. Design considerations to fabricate multifunctional superomniphobic surfaces: a review. Vacuum. 2023;209:111758.
11. Li Y, Hu X, Jin P, Song X. Surface modification to produce superhydrophobic hollow fiber membrane contactor to avoid membrane wetting for biogas purification under pressurized conditions. Separat Purific Technol. 2018;194:222–30.
12. Toh MJ, Oh PC, Chew TL, Ahmad AL. Preparation of polydimethylsiloxane-SiO2/PVDF-HFP mixed matrix membrane of enhanced wetting resistance for membrane gas absorption. Separat Purific Technol. 2020;244:116543.
13. Saleh SM, Tamidi AM, Kadirkhan F, Oh PC. Superhydrophobic membrane for gas-liquid membrane contactor applications. In: Superhydrophobic Coating-Recent Advances in Theory and Applications.. IntechOpen; 2023.
14. Huang A, Chen LH, Chen CH, Tsai HY, Tung KL. Carbon dioxide capture using an omniphobic membrane for a gas-liquid contacting process. J Membr Sci. 2018;556:227–37.
15. Wang X, Xiao C, Liu H, Huang Q, Hao J, Fu H. Poly (vinylidene fluoride-hexafluoropropylene) porous membrane with controllable structure and applications in efficient oil/water separation. Materials. 2018;11(3):443.
16. Tuteja A, Choi W, Mabry JM, McKinley GH, Cohen RE. Robust omniphobic surfaces. Proceed Nat Acad Sci. 2008;105(47):18200–5.
17. Zheng R, Chen Y, Wang J, Song J, Li XM, He T. Preparation of omniphobic PVDF membrane with hierarchical structure for treating saline oily wastewater using direct contact membrane distillation. J Membr Sci. 2018;555:197–205.
18. Kharraz JA, Farid MU, Khanzada NK, Deka BJ, Arafat HA, An AK. Macro-corrugated and nano-patterned hierarchically structured superomniphobic membrane for treatment of low surface tension oily wastewater by membrane distillation. Water Res. 2020;174:115600.
19. Qing W, Wu Y, Li X, Shi X, Shao S, Mei Y, et al. Omniphobic PVDF nanofibrous membrane for superior anti-wetting performance in direct contact membrane distillation. J Membr Sci. 2020;608:118226.

20. Koh E, Lee YT. Preparation of an omniphobic nanofiber membrane by the self-assembly of hydrophobic nanoparticles for membrane distillation. Separ Purific Technol. 2021;259:118134.
21. Zhang X, Liao X, Shi M, Liao Y, Razaqpur AG, You X. Guide to rational membrane selection for oily wastewater treatment by membrane distillation. Desalination. 2023;549:116323.
22. Twibi MF, Othman MH, Sokri MN, Alftessi SA, Adam MR, Meshreghi HD, et al. Novel approach to surface functionalization of mullite-kaolinite hollow fiber membrane using organosilane-functionalized Co3O4 spider web-like layer deposition for desalination using direct contact membrane distillation. Ceram Int. 2022;48(14):21025–36.
23. Li H, Feng H, Li M, Zhang X. Engineering a covalently constructed superomniphobic membrane for robust membrane distillation. J Membr Sci. 2022;644:120124.
24. Chiao YH, Cao Y, Ang MB, Sengupta A, Wickramasinghe SR. Application of superomniphobic electrospun membrane for treatment of real produced water through membrane distillation. Desalination. 2022;528:115602.
25. Erbil HY. Practical applications of superhydrophobic materials and coatings: problems and perspectives. Langmuir. 2020;36(10):2493–509.
26. Toh MJ, Oh PC, Ahmad AL, Caille J. Enhancing membrane wetting resistance through superhydrophobic modification by polydimethylsilane-grafted-SiO2 nanoparticles. Korean J Chem Engin. 2019;36(11):1854–8.
27. Ahmad AL, Hassan AI, Peng LC. Non-solvent influence of hydrophobic polymeric layer deposition on PVDF hollow fiber membrane for CO2 gas absorption. Membranes. 2021;12(1):41.
28. Thürmer MB, Poletto P, Marcolin M, Duarte J, Zeni M. Effect of non-solvents used in the coagulation bath on morphology of PVDF membranes. Mater Res. 2012;15:884–90.
29. Wu X, Zhao B, Wang L, Zhang Z, Li J, He X, et al. Superhydrophobic PVDF membrane induced by hydrophobic SiO2 nanoparticles and its use for CO2 absorption. Separat Purific Technol. 2018;190:108–16.
30. Rosli A, Ahmad AL, Low SC. Enhancing membrane hydrophobicity using silica end-capped with organosilicon for CO2 absorption in membrane contactor. Separat Purific Technol. 2020;251:117429.
31. Wang H, Zhang Z, Wang Z, Zhao J, Liang Y, Li X, et al. Improved dynamic stability of superomniphobic surfaces and droplet transport on slippery surfaces by dual-scale re-entrant structures. Chem Engin J. 2020;394:124871.
32. Prasanna NS, Choudhary N, Singh N, Raghavarao KS. Omniphobic membranes in membrane distillation for desalination applications: a mini-review. Chem Engin J Adv. 2023;14:100486.
33. Bakeri G, Ismail AF, Shariaty-Niassar M, Matsuura T. Effect of polymer concentration on the structure and performance of polyetherimide hollow fiber membranes. J Membr Sci. 2010;363(1–2):103–11.
34. Rosli A, Ahmad AL, Low SC. Anti-wetting polyvinylidene fluoride membrane incorporated with hydrophobic polyethylene-functionalized-silica to improve CO2 removal in membrane gas absorption. Separat Purific Technol. 2019;221:275–85.
35. Rongwong W, Fan C, Liang Z, Rui Z, Idem RO, Tontiwachwuthikul P. Investigation of the effects of operating parameters on the local mass transfer coefficient and membrane wetting in a membrane gas absorption process. J Membr Sci. 2015;490:236–46.
36. Ahmad NA, Noh AM, Leo CP, Ahmad AL. CO2 removal using membrane gas absorption with PVDF membrane incorporated with POSS and SAPO-34 zeolite. Chem Engin Res Des. 2017;118:238–47.
37. Chang PT, Paranthaman S, Rosli A, Low SC. Manipulating membrane hydrophobicity by integrating polythylene-coated fume silica in PVDF membrane. ASEAN Engin J. 2022;12(1):157–64.
38. Pang H, Qiu Y, Sheng W. Long-term stability of PVDF-SiO2-HDTMS composite hollow fiber membrane for carbon dioxide absorption in gas–liquid contacting process. Sci Rep. 2023;13(1):5531.
39. Rongwong W, Jiraratananon R, Atchariyawut S. Experimental study on membrane wetting in gas–liquid membrane contacting process for CO2 absorption by single and mixed absorbents.

Separat Purific Technol. 2009;69(1):118–25.
40. Atchariyawut S, Jiraratananon R, Wang R. Mass transfer study and modeling of gas–liquid membrane contacting process by multistage cascade model for CO2 absorption. Separat Purific Technol. 2008;63(1):15–22.
41. Talavari A, Ghanavati B, Azimi A, Sayyahi S. Preparation and characterization of PVDF-filled MWCNT hollow fiber mixed matrix membranes for gas absorption by Al2O3 nanofluid absorbent via gas–liquid membrane contactor. Chem Engin Res Des. 2020;156:478–94.

